Electronic Supplementary Material (ESI) for Journal of Materials Chemistry A.

Electronic Supporting Information

Superassembly of $NiCoO_x$ Solid Solution Hybrids with a 2D/3D Porous Polyhedron-on-sheet Structure for Multi-functional Electrocatalytic Oxidation

Pin Hao,[a, †, *] Houguang Wen,[a, †] Qian Wang,[a] Liyi Li,[b] Zhenhuan Zhao,[c] Ruirui Xu,[a] Junfeng Xie,[a] Guanwei Cui[a] and Bo Tang[a*]

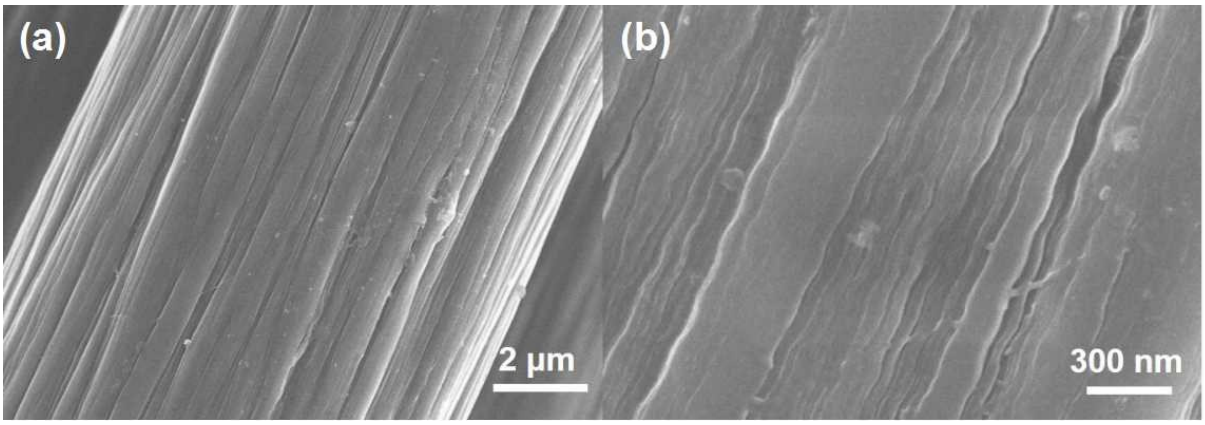

Fig.S1 The SEM image of CC.

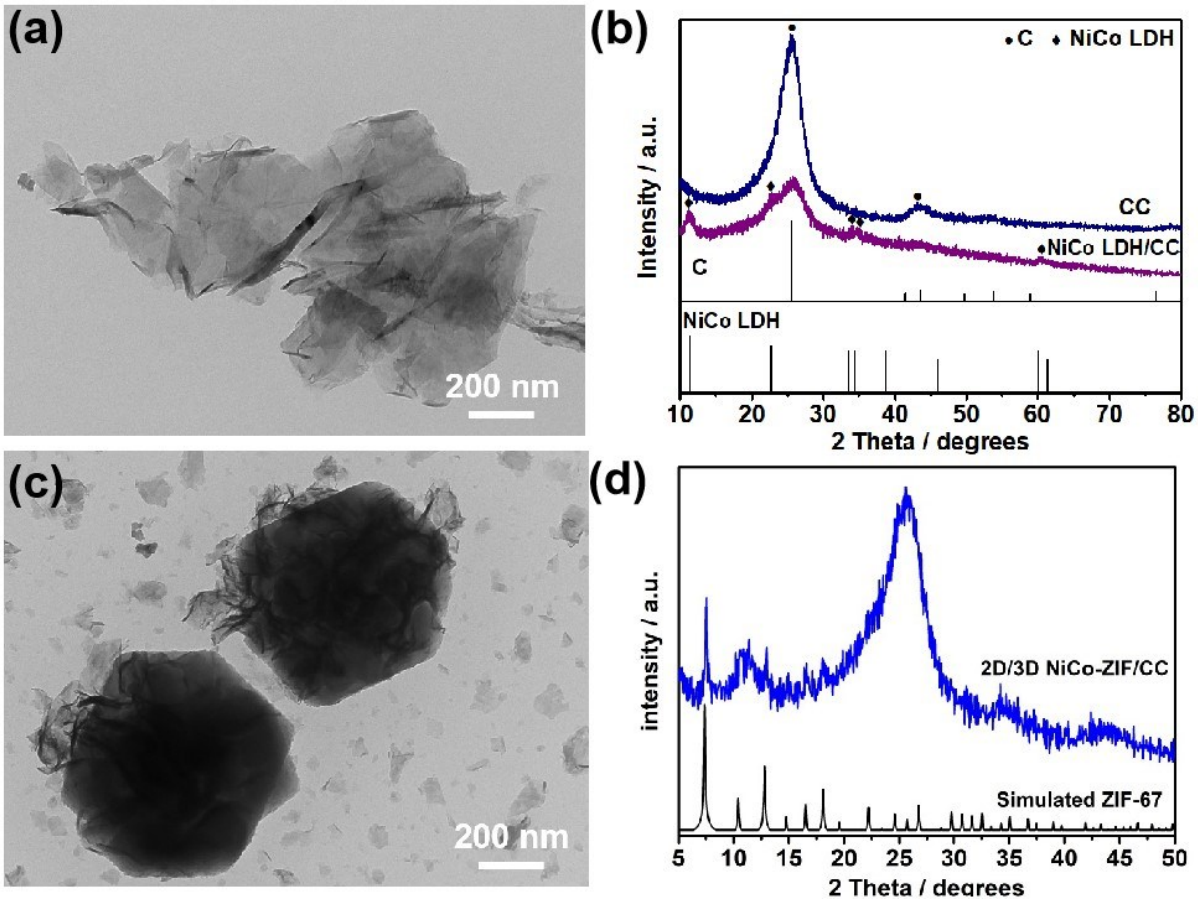

Fig.S2 TEM images and XRD patterns of (a, b) NiCo LDH/CC, (c , d) 2D/3D NiCo-ZIF/CC.

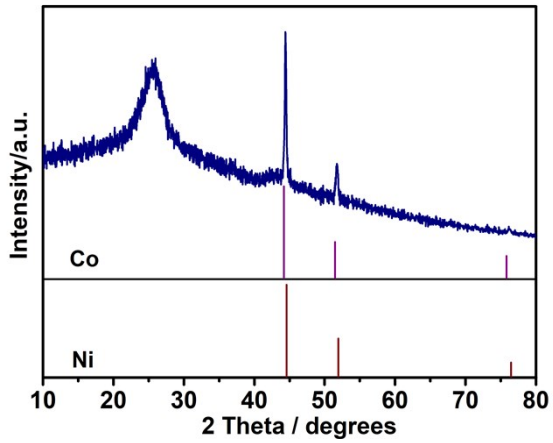

Fig.S3 XRD pattern of NiCo alloys on CC via annealing the 2D/3D NiCo-ZIF/CC at 550 ^{o}C for 1 h under N_2.

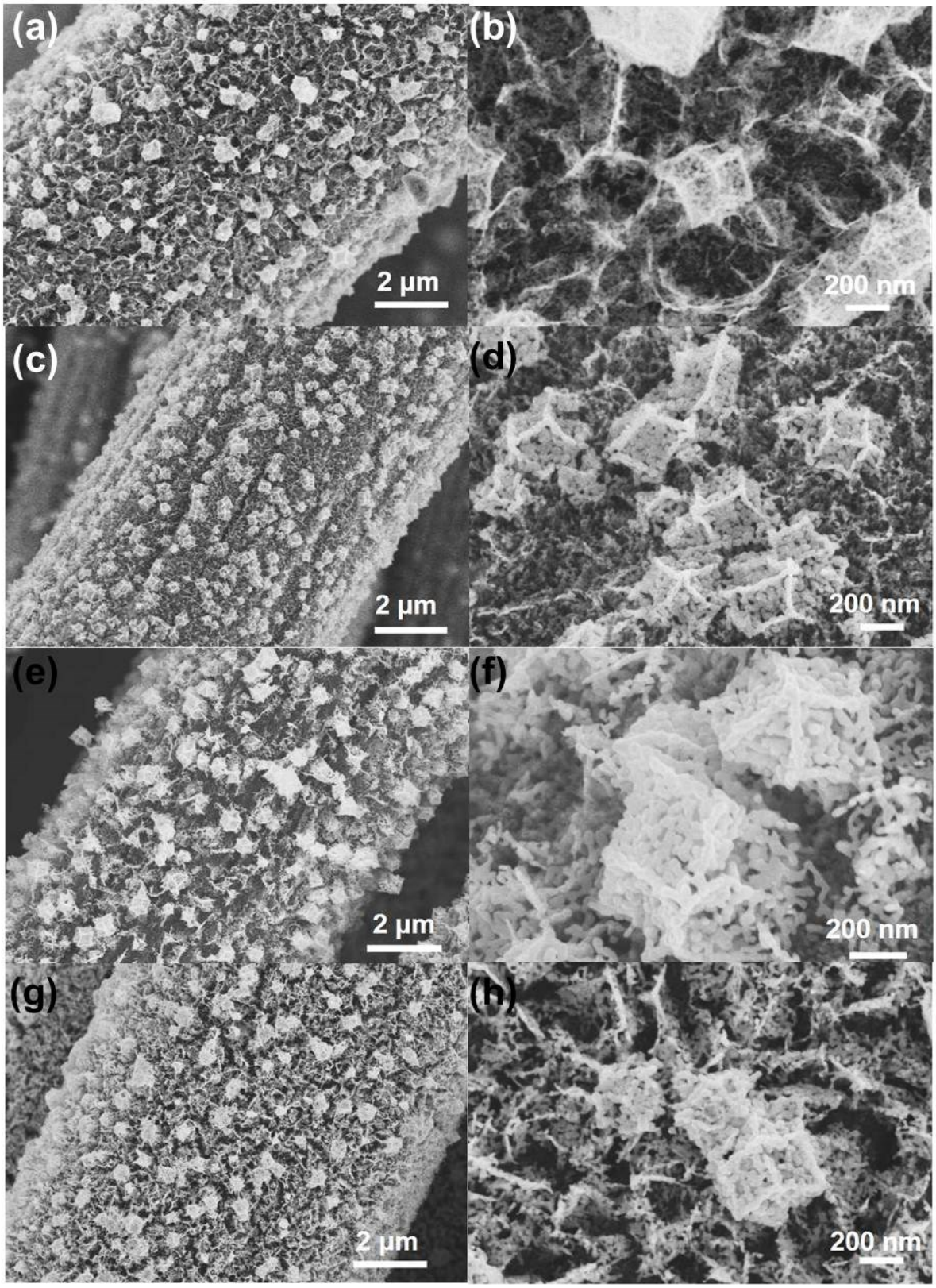

Fig.S4 SEM images of (a, b) CO/CC, (c, d) NCO/CC 1:2, (e, f) NCO/CC 3:4, and (g, h) NCO/CC 4:3.

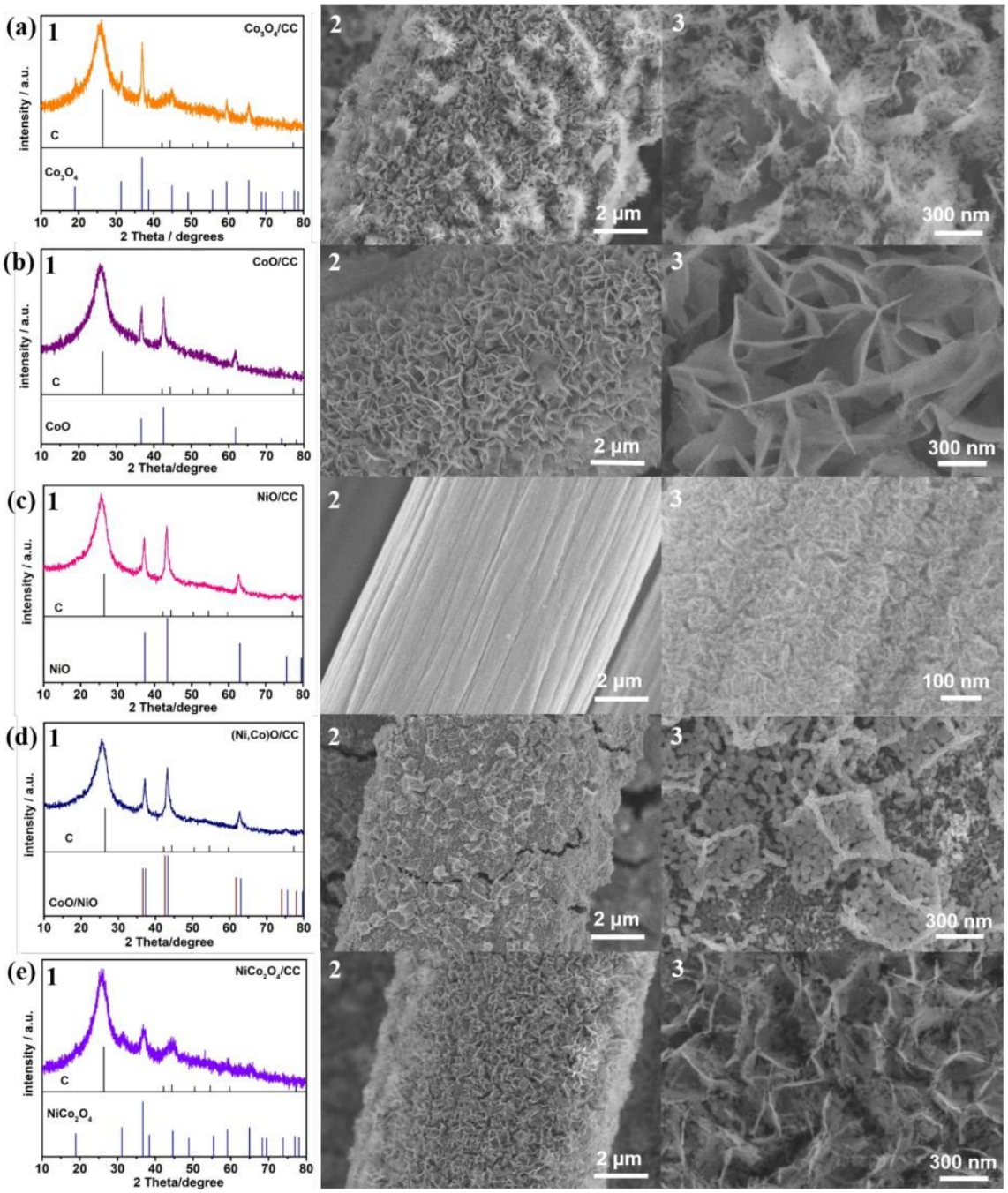

Fig.S5 Phase and morphological characterization of (a) Co_3O_4/CC, (b) CoO/CC, (c) NiO/CC, (d) (Ni, Co)/CC and (e) $NiCo_2O_4$/CC: (1) XRD patterns, (2, 3) SEM images.

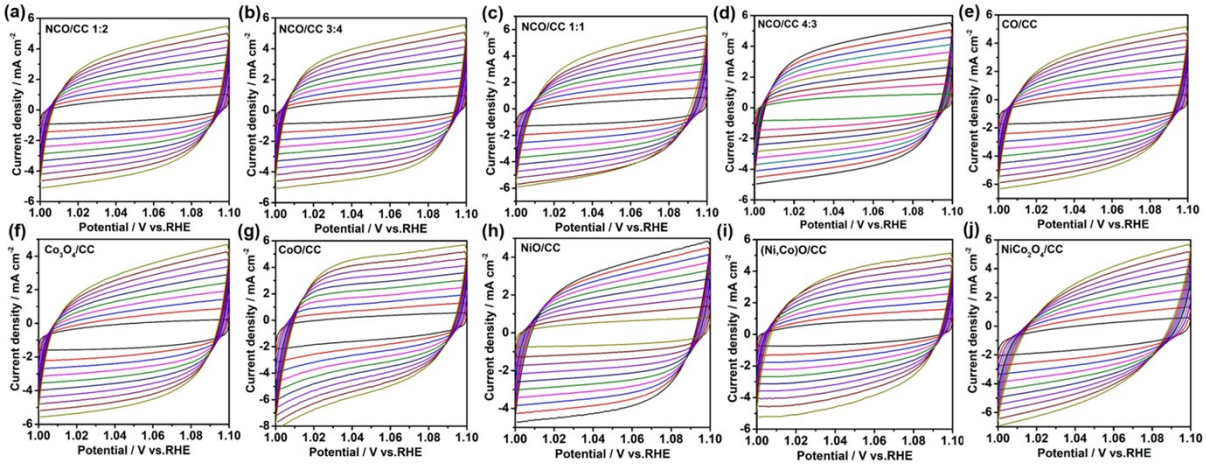

Fig.S6 CV curves of the samples at the various scan rates from 10-100 mV s^{-1} in non-redox region for the calculation of electrochemical double-layer capacitance.

The investigation of the electrochemical surface area (ECSA) of the samples was carried out according to literature.[1] ECSA was estimated by measuring the electrochemical double-layer capacitance. Cyclic voltammetry (CV) was employed at various scan rates from 10 to 100 mV s^{-1} in 1.0-1.1 V vs. RHE region, which could be considered as the double-layer capacitive behavior. The electrochemical double-layer capacitance (C_{dl}) can be calculated based on the CV curves (Fig.S6a-j). The value of C_{dl} is estimated by plotting the ΔJ (J_a-J_c) at 1.05 V vs. RHE against the scan rate, where the slope is twice C_{dl}.

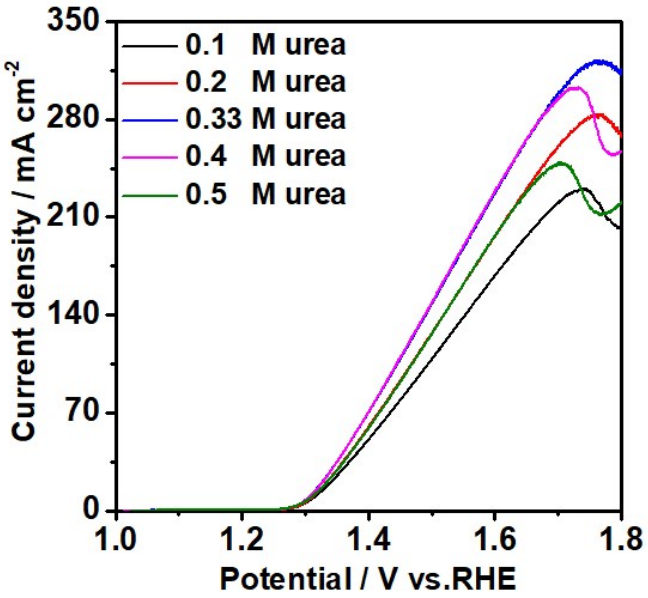

Fig.S7 LSV curves of NCO/CC 1:1 in 1 M KOH solution with different urea concentrations.

From this figure, we can see the optimum concentration of urea to achieve a good catalytic performance is 0.33 M. That is, at lower urea concentrations below 0.33 M, the UOR current density increases as the concentration increases, ascribing to the diffusion-controlled

reaction mechanism. While at concentrations higher than 0.33 M, the UOR current becomes deterioration, since most active sites on the surface of NCO/CC 1:1 are covered by urea and its oxidation intermediates, resulting in the reduced urea oxidation due to the local deficiency of OH^-.[2, 3]

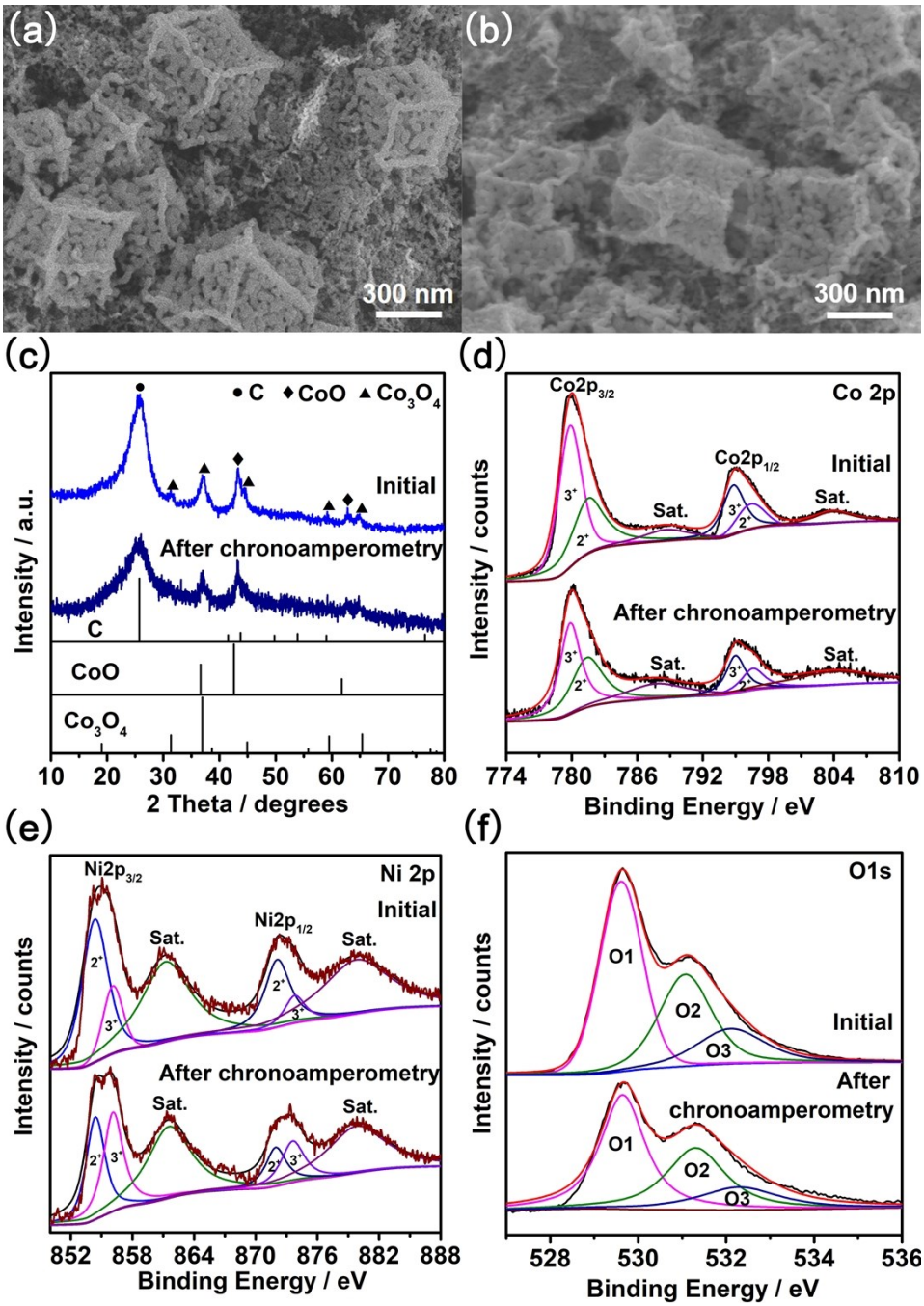

Fig.S8 SEM images, XRD and high-solution XPS spectra of NCO/CC 1:1 before and after chronoamperometric test: SEM of (a) before chronoamperometric test and (b) after chronoamperometric test, (c) XRD, XPS of (d) Co, (e) Ni and (f) O.

Table S1 Comparison of catalytic activity for UOR on different catalysts.

Catalyst	Concentration of Urea (M)	Potential at 10 mA cm^{-2} (V)	Potential at 100 mA cm^{-2} (V)	Reference
$NiMoO_3S$/NF	0.5	1.34	~1.44	Ref.4
$Ni(OH)_2$@NF	0.3	1.35	~1.43	Ref.5
Ni@NCNT-3	0.5	1.38	NA	Ref.6
NiMo@ZnO/NF	0.33	1.41	~1.48	Ref.7
$Ni_{1.6}Co_{0.4}P$/C@HCNs	0.33	1.33	~1.5	Ref.8
$Ni/Ni_{0.2}Mo_{0.8}N/MoO_3$	0.5	1.35	~1.61	Ref.9
Co_xS/Co-MOF	0.5	1.32	~1.44	Ref.10
$Ni/NiO@NC_{400}$	0.33	1.35	NA	Ref.11
CoFeCr LDH/NF	0.33	1.31	~1.55	Ref.12
$NiO/NiCr_2O_4$-2	0.33	~1.35	NA	Ref.13
Co_3Mo_1S-CC	0.5	1.31	~1.5	Ref.14
NiFeRh-LDH	0.33	1.34	~1.47	Ref.15
$NiSe_2$-NiO	0.33	1.33	NA	Ref.16
V_8C_7/CoP-0.18	0.33	1.34	~1.65	Ref.17
MOF-Ni@MOF-Fe-S	0.5	1.34	~1.46	Ref.18
NP-$Ni_{0.70}Fe_{0.30}$	0.33	~1.43	~1.55	Ref.19
Pt/C-NF	0.3	1.37	NA	Ref.20
NCO/CC 1:1	0.33	1.30	1.43	This work

Note: "~" stands for the estimated value from the LSV curves.

Reference

1. J. Xie, J. Zhang, S. Li, F. Grote, X. Zhang, H. Zhang, R. Wang, Y. Lei, B. Pan and Y. Xie, *J. Am. Chem. Soc.,* 2013, **135**, 17881-17888.
2. J. Xie, H. Qu, F. Lei, X. Peng, W. Liu, L. Gao, P. Hao, G. Cui and B. Tang, *J. Mater. Chem. A*, 2018, **6**, 16121-16129.
3. P. Hao, W. Zhu, L. Li, J. Tian, J. Xie, F. Lei, G. Cui, Y. Zhang and B. Tang, *Electrochim. Acta*, 2020, **338**, 135883.
4. W. Han, X. Li, L. Lu, T. Ouyang, K. Xiao and Z. Liu, *Chem. Commun.,* 2020, **56,** 11038-11041.

5. L. Xia, Y. Liao, Y. Qing, H. Xu, Z. Gao, W. Li, Y. Wu, *ACS Appl. Energy Mater.,* 2020, **3**, 2996-3004.
6. Q. Zhang, F. Kazim, S. Ma, K. Qu, M. Li, Y. Wang, H. Hu, W. Cai and Z. Yang, *Appl. Catal. B- Environ.,* 2020, **280,** 119436.
7. J. Cao, H. Li, R. Zhu, L. Ma, K. Zhou, Q. Wei and F. Luo, *J. Alloys Compd.,* 2020, **844,** 155382.
8. S. Rezaee and S. Shahrokhian, *Nanoscale,* 2020, **12,** 16123-16135.
9. R. Li, S. Li, M. Lu, Y. Shi, K. Qu and Y. Zhu, *J. Colloid Interface Sci.,* 2020, **571,** 48-54.
10. H. Xu, K. Ye, K. Zhu, J. Yin, J. Yan, G. Wang and D. Cao, *Inorg. Chem. Front.,* 2020, **7,** 2602-2610.
11. X. Ji, Y. Zhang, Z. Ma and Y. Qiu, *ChemSusChem*, 2020, **13**, 5004-5014.
12. Z. Wang, W. Liu, Y. Hu, M. Guan, L. Xu, H. Li, J. Bao and H. Li, *Appl. Catal. B-Environ.,* 2020, **272**, 118959.
13. Y. Liu, M. Huang, J. Zhao, M. Lu, X. Zhou, Q. Lin, P. Wang and J. Zhu, *J. Electrochem. Soc.,* 2020, **167**, 066520.
14. P. Li, Z. Zhuang, C. Du, D. Xiang, F. Zheng, Z. Zhang, Z. Fang, J. Guo, S. Zhu and W. Chen, *ACS Appl. Mater. Interfaces,* 2020, **12,** 40194-40203.
15. H. Sun, W. Zhang, J. Li, Z. Li, X. Ao, K. Xue, K. K. Ostrikov, J. Tang and C. Wang, *Appl. Catal. B- Environ.*, 2021, **284**, 119740.
16. Z. Liu, C. Zhang, H. Liu and L. Feng, *Appl. Catal. B- Environ.*, 2020, **276**, 119165.
17. L. Wu, M. Zhang, Z. Wen and S. Ci, *Chem. Eng. J.,* 2020, **399,** 125728.
18. H. Xu, K. Ye, K. Zhu, J. Yin, J. Yan, G. Wang and D. Cao, *Dalton Trans.,* 2020, **49**, 5646-5652.
19. C. Zhen, T. Zhou, X. Ma, Y. Shen, Q. Deng, W. Zhang and Y. Zhao, *ACS Sustainable Chem. Eng.*, 2020, **29**, 11007-11015.
20. L. Xia, Y. Liao, Y. Qing, H. Xu, Z. Gao, W. Li and Y. Wu, *ACS Appl. Energy Mater.,* 2020, **3**, 2996-3004.